16th World Conference on Earthquake Engineering, 16WCEE 2017
Santiago Chile, January 9th to 13th 2017
Paper N° 1275
Registration Code: S-R1461195881

Dynamic Characteristics of Buildings Constructed by Pile Top Seismic Isolation System Considering Nonlinearity of Laminated Rubber Bearing

T. Yamauchi[(1)], H. Kitamura[(2)], M. Nagano[(3)], T. Sato[(4)], K. Suzuki[(5)]

[(1)] *Technical Research Institute, Asanuma Corporation, yamauchi-toyohide@asanuma.co.jp*
[(2)] *Professor, Tokyo University of Science, kita-h@rs.noda.tus.ac.jp*
[(3)] *Professor, Tokyo University of Science, nagano-m@rs.noda.tus.ac.jp*
[(4)] *Associate Professor, Kyushu University, sato@arch.kyushu-u.ac.jp*
[(5)] *Assistant Professor, Tokyo University of Science, suzuki-k@rs.tus.ac.jp*

Abstract

A pile top seismic isolation system is used for constructing base-isolated buildings. In this system, seismic isolators are set on the pile's top directly, and piles are connected with thin foundation girders or a mat slab. In recent years, many logistics centers in Japan have been constructed using this system because it enables significant cost reductions in underground construction.

However, this system does have some problems. For example, the laminated rubber bearing's bottom part easily undergoes bending rotation because the thin foundation girders have low stiffness. This tendency becomes more pronounced in the case of soft ground. If bending rotation occurs, the laminated rubber bearing's horizontal stiffness reduces under the influence of the horizontal component of the axial load, and its inflection point moves downward from the center height of the device (usually, the point does not move). This, in turn, significantly affects the structural characteristics of the pile top seismic isolation building. In addition, it has been noted that the horizontal stiffness and rotational stiffness of the laminated rubber bearing show deformation-dependent nonlinearity.

In order to evaluate such special behaviors of the pile top seismic isolation building appropriately, it is required to consider the dynamic soil–structure interaction and the nonlinearity of the laminated rubber bearing. In particular, analytical models that can consider the geometric nonlinearity and various nonlinear characteristics caused by the bending rotation of a laminated rubber bearing have been proposed. However, highly specialized knowledge is needed to use these models, and such knowledge is difficult to incorporate into general-purpose design software. Therefore, it's not considered sufficiently their effects in conventional structural design at present.

This paper describes the seismic behaviors of laminated rubber bearings in a pile top seismic isolation buildings through numerical experiments by considering the nonlinearity of the laminated rubber bearing and the dynamic soil–structure interaction.

The parametric analytical study is performed by the elasto-plastic earthquake response analysis. The analytical model is of the fishbone type, and it represents one span of the logistics center. It consists of a superstructure, seismic isolated layer, thin foundation girders, a pile, soil-pile springs, and free field. The laminated rubber bearing model is based on Haringx's theory, and this model is constructed using three matrices: horizontal stiffness matrix, geometric nonlinear matrix, and rotational stiffness matrix.

The following conclusions are obtained through numerical experiments on the pile top seismic isolation building.

1. The dynamic characteristics of the laminated rubber bearing are quantitatively evaluated depending on the characteristics of the substructure. In addition, it is shown that their values are affected by the influence of the correlation between the horizontal deformation and the rotational angle of the laminated rubber bearing.
2. It is clarified that the dynamic characteristics of the laminated rubber bearing can be evaluated using a simple indicator called the rotational stiffness ratio. In addition, their values are evaluated by considering the dependency of the axial load on the laminated rubber bearing.

Keywords: Pile Top Seismic Isolation System, Laminated Rubber Bearing, Nonlinearity, Dynamic Characteristic

1. Introduction

A pile top seismic isolation system is used for constructing base-isolated buildings. In this system, seismic isolators are set on the pile's top directly, and piles are connected with thin foundation girders or a mat slab. In recent years, many logistics centers in Japan have been constructed using this system because it enables significant cost reductions in underground construction.

However, this system does have some problems. For example, the laminated rubber bearing's bottom part easily undergoes bending rotation because the thin foundation girders have low stiffness. This tendency becomes more pronounced in the case of soft ground. If bending rotation occurs, the laminated rubber bearing's horizontal stiffness reduces under the influence of the horizontal component of the axial load, and its inflection point moves downward from the center height of the device (usually, the point does not move) [1, 2]. If the inflection point moves, the sharing ratio of the bending moment between the upper and the lower structural members becomes uneven. This, in turn, significantly affects the structural characteristics of the pile top seismic isolation building. In addition, it has been noted that the horizontal stiffness and rotational stiffness of the laminated rubber bearing show deformation-dependent nonlinearity [2].

Recently, analytical models that can consider the geometric nonlinearity and various nonlinear characteristics caused by the bending rotation of a laminated rubber bearing have been proposed [2, 3]. However, highly specialized knowledge is needed to use these models, and such knowledge is difficult to incorporate into general-purpose design software.

This paper describes the evaluation results of the dynamic characteristics of laminated rubber bearings by earthquake response analysis considering the nonlinearity of the laminated rubber bearing and the dynamic soil – structure interaction.

2. Outline of Dynamic Analysis

2.1 Analytical Model of Pile Top Seismic Isolation Building

Figure 1 shows the dynamic analytical model. The analytical model is of the fishbone type, and it represents one span of the pile top seismic isolation building. It consists of a superstructure, seismic isolated layer, thin foundation girders, a pile, soil-pile springs, and free field.

The superstructure model comprises a mixed structure (RC columns and steel girders). All frames of the superstructure model are elastic beam elements. The compressive strength of concrete f_c at RC columns is 36 N/mm^2, and Young's modulus is calculated from the compressive strength [4]. Young's modulus of steel is 205000 N/mm^2 [5]. The seismic isolated layer is constructed using a steel damper and a laminated rubber bearing. The steel damper has a normal bilinear model; its yield displacement is 2 cm, and its yield shear force is 240.4 kN (Figure 1). The laminated rubber bearing is a natural rubber bearing; an overview of its parameters is shown in Table 1. The axial load that acts on the laminated rubber bearing is 8000 kN (axial stress: 10.2 N/mm^2). The laminated rubber bearing model is described in detail later.

The thin foundation girder, pile, and ground conditions are the parameters used in the dynamic analysis, because these have various influences on the bending rotation of the laminated rubber bearing. The thin foundation girders have an RC structure. The model of the thin foundation girders contains elastic beam elements. The compressive strength f_c of concrete is 36 N/mm^2. Table 2 shows the section size of the thin foundation girder. Table 2 also shows the relative stiffness ratio of the thin foundation girder (FG/1G). Two types of piles are used: steel pile and RC pile (Table 2). The model of the pile contains elastic beam elements.

The parameters of the free field and soil-pile springs are the N-value of the ground. The velocity V_S of the secondary wave of the ground is calculated using the N-value (Table 2) [6]. The stiffness k_{fs} of the soil-pile springs is calculated using Eq.(1), which was proposed by Francis [7].

$$k_{fS} = \frac{1.3E_S}{1-\nu_S^2}\left(\frac{E_S B^4}{E_p I_p}\right)^{1/12} H\beta_H^{4/3},\ \left(E_S = 2(1+\nu_S)\rho V_S^2\right) \tag{1}$$

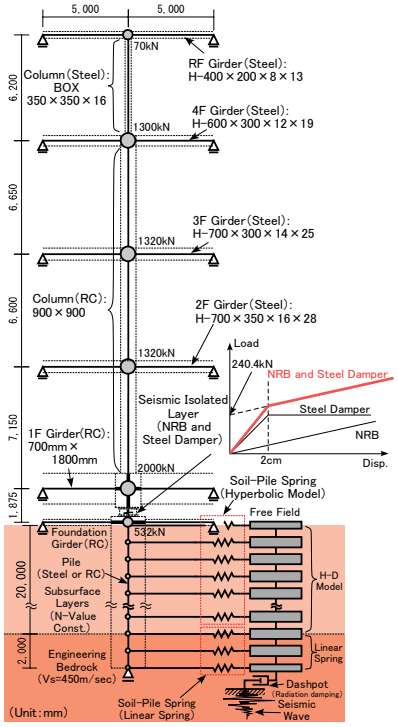

Fig.1 – Analytical model

Table 1 – Overview of NRB

Shear modulus : G(N/mm^2)	0.39
Young's modulus : E_0(N/mm^2)	1.17
Correction factor : κ	0.85
Bulk modulus : E_∞(N/mm^2)	1961
Outer diameter : D(mm)	1000
Inner diameter : d(mm)	25
Total rubber thickness : $n \cdot t_r$(mm)	200
Primary shape factor : S_1	36.4
Secondary shape factor : S_2	5.00
Bending elastic modulus : E_{rb}(N/mm^2) $E_{rb}=\frac{E_b \cdot E_\infty}{E_b+E_\infty}, \left(E_b=\left(1+\frac{2}{3}\kappa S_1^2\right)\right)$	606.8

Table 2 – Parameters of dynamic analysis

Foundation girder	Pile	N-value of ground
Pin joint (0.0)	Steel Pile (B:1200mm, t:19mm, E_s:205000N/mm^2)	1:Clay (V_s= 100 m/s)
B:1000mm×D:350mm (0.011)		5:Sand (V_s= 137 m/s)
B:2000mm×D:350mm (0.021)		10:Sand (V_s= 172 m/s)
B:3000mm×D:350mm (0.032)	RC Pile (B:2000mm, f_c=36N/mm^2)	15:Sand (V_s= 197 m/s)
B:4000mm×D:350mm (0.042)		20:Sand (V_s= 217 m/s)
RC structure f_c=36N/mm^2 The numbers in paretheses are the relative stiffness ratio	-	Vs calculated by N-value

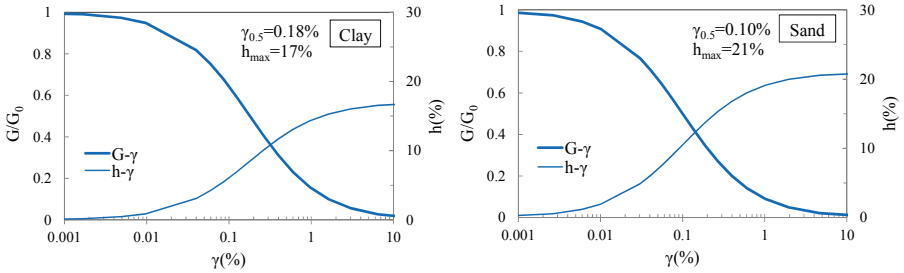

Fig.2 – Strain dependency of ground (G-γ, h-γ)

E_s and ν_S represent Young's modulus and Poisson's ratio (ν_S = 0.48) of the ground, respectively, and B, E_p, and I_p represent the diameter, Young's modulus, and geometrical moment of inertia of a pile. H represents the thickness of subsurface layers that are partitioned. β_H represents the coefficient of a pile group. ρ represents the soil density (ρ = 1.8t/m^3). V_S of engineering bedrock is 450 m/s. The soil-pile springs in the subsurface layers have a hyperbolic model. The ultimate strength of the subgrade reactions in the subsurface layers is calculated using Broms's equation [7]. The free field is a large lumped mass model with cross-sectional area of 10000m^2. The subsurface layers have an H-D model [8], and Figure 2 shows the strain dependency [9].

2.2 Analytical Model of Laminated Rubber Bearing Considering Nonlinearity

In this paper, the analytical model of the laminated rubber bearing is based on Miyama's method [2]. Miyama defined the deformation of a laminated rubber bearing as shown in Figure 3 and proposed the stiffness matrix of the laminated rubber bearing based on Haringx's theory [10]. The stiffness matrix is constructed using three matrices: horizontal stiffness matrix [K_H], geometric nonlinear matrix [K_P], and rotational stiffness matrix [K_R] (Eq.(2)).

$$\begin{Bmatrix} Q_A \\ M_A \\ Q_B \\ M_B \end{Bmatrix} = \begin{bmatrix} K_H + & K_P & + K_R \end{bmatrix} \begin{Bmatrix} x_A \\ \theta_A \\ x_B \\ \theta_B \end{Bmatrix}$$

$$= \left[K_h \begin{bmatrix} 1 & -h/2 & -1 & -h/2 \\ & h^2/4 & h/2 & h^2/4 \\ & & 1 & h/2 \\ & sym. & & h^2/4 \end{bmatrix} + P \begin{bmatrix} 0 & -1/2 & 0 & -1/2 \\ & h/4 & 1/2 & h/4 \\ & & 0 & 1/2 \\ & sym. & & h/4 \end{bmatrix} + K_r \begin{bmatrix} 0 & 0 & 0 & 0 \\ & 1 & 0 & -1 \\ & & 0 & 0 \\ & sym. & & 1 \end{bmatrix} \right] \begin{Bmatrix} x_A \\ \theta_A \\ x_B \\ \theta_B \end{Bmatrix} \quad (2)$$

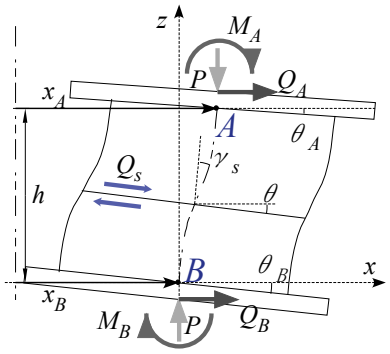

Fig.3 – Deformation of laminated rubber bearing

Q_A and Q_B, M_A and M_B, x_A and x_B, and θ_A and θ_B represent the shear forces, bending moments, horizontal displacements, and bending rotational angles at points A and B, respectively, in Figure 3. P represents the axial load that acts on the laminated rubber bearing (= 8000 kN), and h represents the total height of the laminated rubber bearing (= 400 mm).

It is possible to consider the geometric nonlinearity (P-Δ effect and the influence of the horizontal component of the axial load) using the matrix $[K_P]$. K_h represents the horizontal stiffness of the laminated rubber bearing considering the dependency of the axial load (Eq.(3)). P_{cr} and A_e represent the axial buckling load and effective plane area of the laminated rubber bearing, respectively. K_r represents the rotational stiffness of the laminated rubber bearing considering the dependency of the axial load and the dependency of the horizontal displacement and material nonlinearity (Eq.(4)). I_e represents the effective geometrical moment of inertia of the laminated rubber bearing.

$$K_h = K_s\left\{1-\left(\frac{P}{P_{cr}}\right)^2\right\}, \quad \left(K_s = \frac{G\cdot A_e}{n\cdot t_r}\right) \tag{3}$$

$$K_r = K_{rc}\left\{1-\left(\frac{P}{P_{cr}}\right)^2\right\}\phi_{rc}\cdot\phi_\sigma, \quad \left(K_{rc} = \frac{E_{rb}\cdot I_e}{n\cdot t_r}\right) \tag{4}$$

ϕ_{rc} represents the dependency of the horizontal displacement (Eq.(5)); it represents the ratio of the geometrical moment of inertia of the overlapping part (upper and lower surfaces) and total area (Figure 4).

$$\phi_{rc} = \frac{4}{\pi}\left(\frac{1}{2}\theta_d + 2\theta_d\cos^2\theta_d - \frac{13}{6}\sin^3\theta_d\cos\theta_d - \frac{5}{2}\sin\theta_d\cos^3\theta_d\right), \quad \left(\cos\theta_d = \frac{x}{D}\right) \tag{5}$$

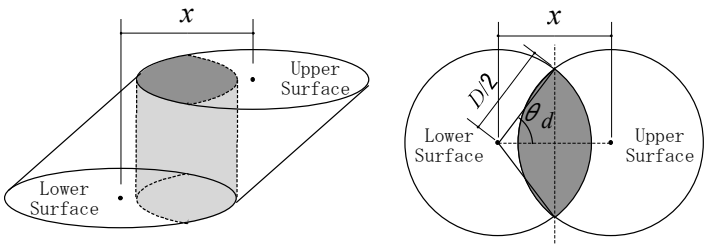

Fig.4 – Overlapping part of upper and lower surfaces of laminated rubber bearing

ϕ_σ represents the material nonlinearity (Eqs.(6) and (7)). Z and σ_y represent the section modulus and tensile yield stress of the laminated rubber bearing, respectively. θ_y represents the rotational angle at which the tensile stress of the outermost laminated rubber bearing reaches σ_y (Eq.(8)). α and β are parameters that are related to the shape of ϕ_σ ($\alpha = 10$, $\beta = 40$ [11]). Figure 5 shows the shapes of ϕ_{rc} and ϕ_σ.

$$\phi_\sigma = 1 \qquad \left(|\theta| \le \theta_y, \theta = \theta_A - \theta_B\right) \tag{6}$$

$$\phi_\sigma = \frac{1}{1+\frac{\alpha}{\beta}\left(\left|\frac{\theta}{\theta_y}\right|-1\right)^{\frac{1+\alpha}{\alpha}}} \qquad \left(|\theta| > \theta_y\right) \tag{7}$$

$$\theta_y = \frac{Z\left(P/A+\sigma_y\right)}{K_h h^2/4 + PH/4 + K_r} \tag{8}$$

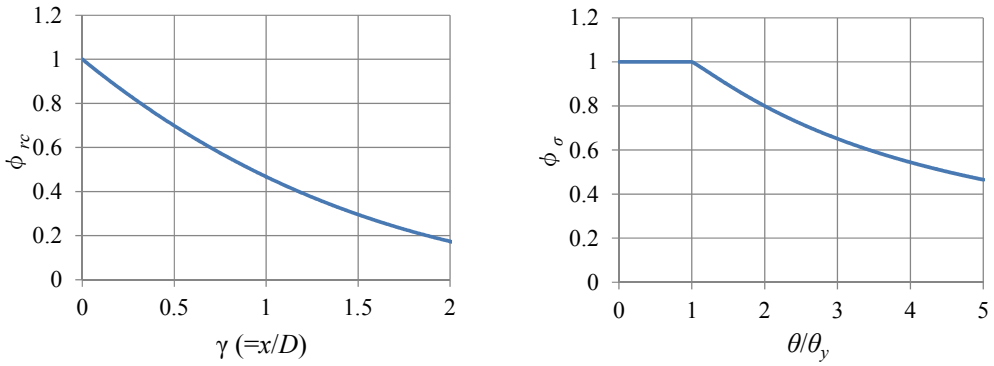

(a) Dependency of horizontal displacement (b) Material nonlinearity

Fig.5 – Nonlinearity of the rotational stiffness K_r

2.3 Seismic Wave

The seismic wave used in the dynamic analysis is simulated using the response spectrum on engineering bedrock of the building standard law in Japan. The response velocity spectrum S_v level when the damping ratio is h = 0.05 is 0.8 m/s. This wave is simulated with a random phase. Figure 6 shows the time history and response velocity spectrum of the seismic wave.

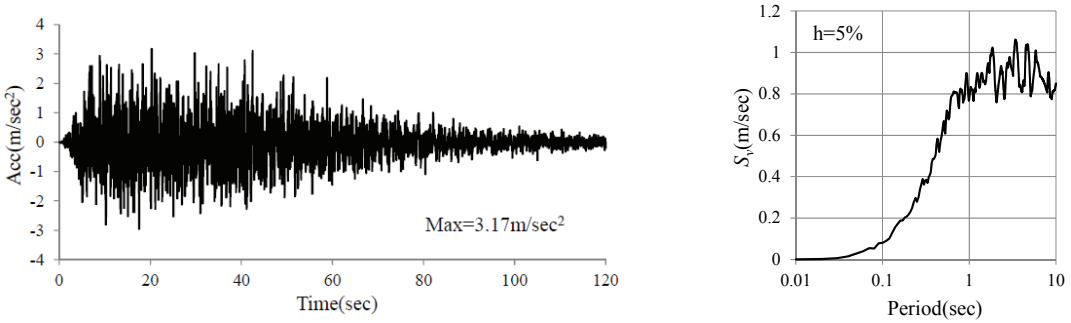

(a) Time history (b) Response velocity spectrum

Fig.6 – Seismic wave

3. Results of Dynamic Analysis

3.1 Results of Eigenvalue Problem

Figure 7 shows the mode shapes derived by the eigenvalue problem (N-value: 10, breadth of thin foundation girder: 2 m). In this case, the stiffness of the seismic isolated layer is the equivalent stiffness at which the shear strain is 100%, and the stiffness of the free field's shear springs is the equivalent stiffness based on the shear strain of the ground. The 1st mode is caused by the shear deformation of the seismic isolated layer. The 2nd mode is caused by the ground's vibration. Table 3 shows the list of natural periods (breadth of thin foundation girder: 2 m).

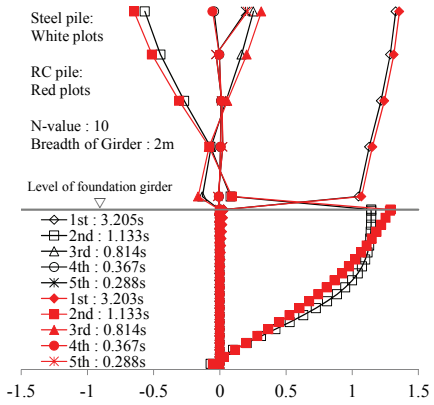

Fig.7 – Mode shapes

Table 3 – List of natural periods (s)

	N-value	1st	2nd	3rd	4th	5th
Steel Pile	1	3.265	2.383	0.815	0.582	0.367
	5	3.225	2.058	0.814	0.465	0.367
	10	3.205	1.133	0.814	0.367	0.288
	15	3.197	0.882	0.814	0.367	0.288
	20	3.192	0.813	0.685	0.367	0.288
RC Pile	1	3.275	2.382	0.816	0.582	0.367
	5	3.225	2.057	0.814	0.466	0.367
	10	3.203	1.133	0.814	0.367	0.288
	15	3.194	0.882	0.813	0.367	0.288
	20	3.189	0.813	0.685	0.367	0.288

3.2 Horizontal Stiffness of Laminated Rubber Bearing

Figure 8 shows an example of the hysteresis loop (shear force–horizontal deformation relation) of the laminated rubber bearing. This figure also shows the hysteresis loops that are calculated using the horizontal stiffness matrix $[K_H]$ and geometric nonlinear matrix $[K_P]$. It has been noted that the horizontal stiffness of the laminated rubber bearing is reduced by the rotation of the bottom part. As shown in Figure 8, the horizontal stiffness of the laminated rubber bearing is reduced by the negative hysteresis loop of the geometric nonlinear matrix $[K_P]$.

The equivalent horizontal stiffness K_{eq} of the laminated rubber bearing is derived by the hysteresis loop using the least squares method. Figure 9 shows K_{eq}/K_h, which is the ratio of the equivalent horizontal stiffness K_{eq} and the horizontal stiffness K_h (Eq.(3)) with no rotational deformation. In this figure, the horizontal axis shows the relative stiffness ratio of the thin foundation girder (FG/1G). As shown in this figure, the reduction rate of K_{eq}/K_h is large if the N-value is small. For a steel pile, the maximum reduction rate of K_{eq}/K_h becomes ~13%. On the other hand, for an RC pile, the maximum reduction rate of K_{eq}/K_h becomes only 2%.

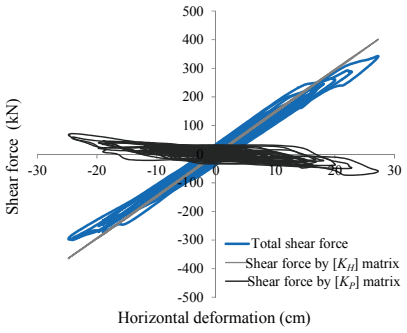

Fig.8 – Hysteresis loop of laminated rubber bearing

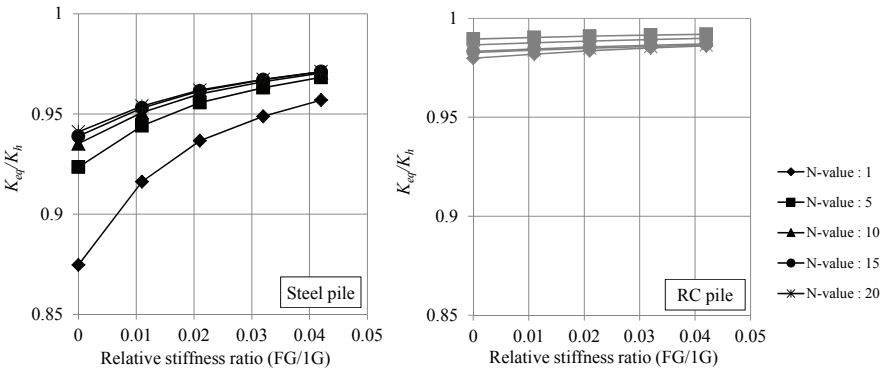

Fig.9 – Relationship of K_{eq}/K_H and relative stiffness ratio (FG/1G)

3.3 Distribution Ratio of Bending Moment of Laminated Rubber Bearing

For pile top seismic isolation buildings, the relationship between the bending moments of the laminated rubber bearing and the three types of matrices in Eq.(2) ($[K_H]$, $[K_P]$, and $[K_R]$) is shown in Figure 10. As shown in this figure, the horizontal stiffness matrix $[K_H]$ and geometrical nonlinear matrix $[K_P]$ distribute the bending moment to the upper and lower sides of the laminated rubber bearing evenly. On the other hand, because the bending moment caused by the rotational stiffness matrix $[K_R]$ has a uniform distribution, the inflection point of the laminated rubber bearing moves downward. As a result, the upper and lower side bending moments of the laminated rubber bearing become uneven. To quantitatively evaluate the distribution of the bending moment of the laminated rubber bearing caused by the movement of the inflection point, the ratio of the bending moment M_A of the upper side of the laminated rubber bearing and the bending moment M_0 with no rotational deformation is given by Eq.(9).

$$\alpha_M = \frac{M_A}{M_0} \tag{9}$$

With regard to the laminated rubber bearing, Figure 11 shows an example of the graph overlapping the time history data of the horizontal deformation and the time history data of α_M. As shown in this figure, when the horizontal deformation crosses the horizontal axis, the value of α_M varies greatly. This phenomenon occurs because there are cases in which the rotational deformation of the laminated rubber bearing is large even if its horizontal deformation is almost zero. This can be understood from Figure 10.

On the other hand, as shown in Figure 11, when the horizontal deformation is large, the value of α_M becomes stable. In actual structural design, the value of α_M becomes important when the bending moments caused by the P-Δ effect and the shear force of the seismic isolated layer are large. In other words, the value of α_M becomes important only when the horizontal deformation of the laminated rubber bearing is large.

Therefore, for $\delta_{\max}$, which represents the maximum horizontal deformation of the laminated rubber bearing, α_M is evaluated by averaging the α_M data when the horizontal deformation of the laminated rubber bearing is more than $0.9 \times \delta_{\max}$.

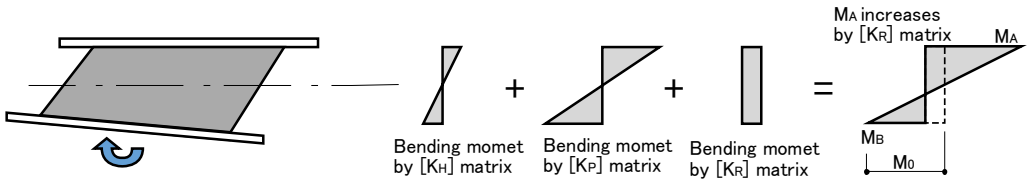

Fig.10 –Bending moments with three types of matrices in Eq.(2)

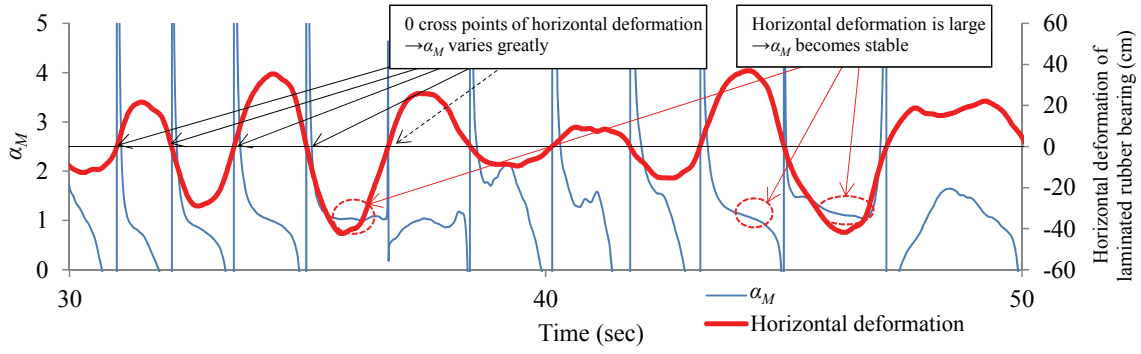

Fig.11 – Relationship between α_M and horizontal deformation of laminated rubber bearing

Figure 12 shows the relationship of α_M (distribution ratio of bending moment of laminated rubber bearing) and the relative stiffness ratio of the thin foundation girder (FG/1G). As shown in this figure, for a steel pile, the maximum value of α_M becomes ~1.5. On the other hand, for an RC pile, the maximum value of α_M becomes only ~1.08.

Figure 13 shows an example of the orbit representing the relationship of the rotational angle and the horizontal deformation in the laminated rubber bearing. The high correlation between the two can be seen for a steel pile. However, almost no correlation is seen for an RC pile. In the pile top seismic isolation building, the correlation of the horizontal deformation and the rotational angle of the laminated rubber bearing varies depending on the characteristics of the substructure. The difference of K_{eq}/K_h and α_M according to the type of pile is also due to this correlation.

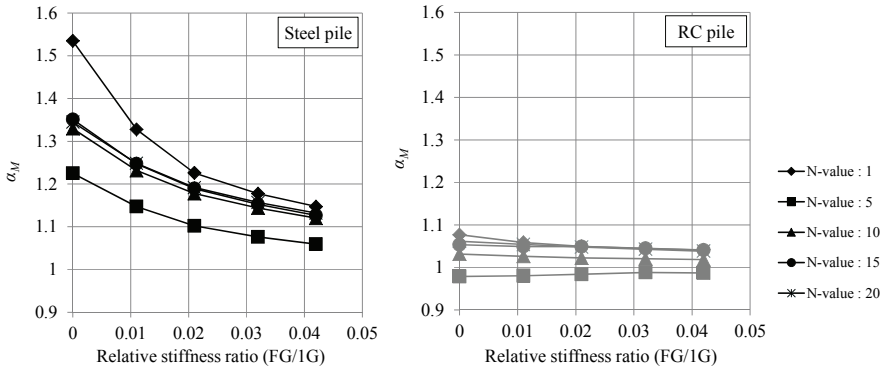

Fig.12 – Relationship of α_M and relative stiffness ratio (FG/1G)

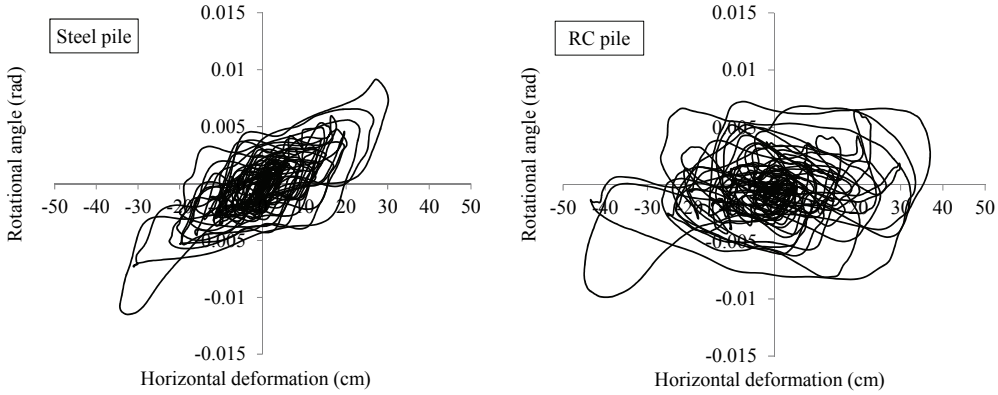

Fig.13 – Orbit of rotational angle and horizontal deformation in laminated rubber bearing
(N-value: 1, breadth of thin foundation girder: 2 m)

4. Evaluation of Dynamic Characteristics of Laminated Rubber Bearing

4.1 Evaluation Using Rotational Stiffness Ratio

This chapter proposes that the dynamic characteristics of the laminated rubber bearing be evaluated using simple indicators such as the rotational stiffness ratio [1].

Because the stiffness of the 1F girder is sufficiently high, it is considered that the upper side of the laminated rubber bearing does not rotate (i.e., rotational angle $\theta_A = 0$). Using the stiffness matrices in Eq.(2), the shear force Q_A that acts on the upper side of the laminated rubber bearing is formulated by Eq.(10).

$$Q_A = K_h\left(x_A - x_B\right) - \frac{K_h \cdot h}{2}\theta_B - \frac{P}{2}\theta_B \tag{10}$$

$\delta = x_A - x_B$, the equivalent horizontal stiffness K_{eq} considering the rotational deformation of the laminated rubber bearing is formulated by Eq.(11), and K_{eq}/K_h (ratio between the equivalent horizontal stiffness K_{eq} and the horizontal stiffness K_h (Eq.(3)) with no rotational deformation) is formulated by Eq.(12).

$$K_{eq} = \frac{Q_A}{\delta} = K_h - \frac{1}{2}\left(K_h \cdot h + P\right)\frac{\theta_B}{\delta} \tag{11}$$

$$\frac{K_{eq}}{K_h} = 1 - \frac{1}{2 \cdot K_h}\left(K_h \cdot h + P\right)\frac{\theta_B}{\delta} \tag{12}$$

Using the stiffness matrices in Eq.(2), the bending moment M_A that acts on the upper side of the laminated rubber bearing is formulated by Eq.(13). When the rotational deformation of the laminated rubber bearing does not occur, the bending moment M_0 of the laminated rubber bearing is formulated by Eq.(14). Therefore, the distribution ratio α_M of the bending moment of the laminated rubber bearing is formulated by Eq.(15).

$$M_A = -\frac{K_h \cdot h + P}{2} \cdot \delta + \frac{K_h \cdot h^2 + P}{4}\theta_B - K_r\theta_B \tag{13}$$

$$M_0 = -\frac{K_h \cdot h + P}{2} \cdot \delta \tag{14}$$

$$\alpha_M = \frac{M_A}{M_0} = 1 + \frac{1}{2}\left(\frac{4 \cdot K_r}{K_h \cdot h + P} - h\right)\frac{\theta_B}{\delta} \tag{15}$$

When the axial load P on the laminated rubber bearing is constant, the unknown value in Eq.(12) is θ_B / δ. The unknown values in Eq.(15) are θ_B / δ, ϕ_{rc}, and ϕ_σ (Eq.(4)).

Kobayashi et al. proposed a simple indicator called the rotational stiffness ratio, and they quantitatively evaluated the characteristics of the laminated rubber bearing through static analysis [1]. The rotational stiffness ratio K_{rc}/K_B is an indicator that divides the rotational stiffness K_{rc} (Eq.(4)) of the laminated rubber bearing by the rotational stiffness K_B of the substructure. Figure 14 shows the outline of the rotational stiffness ratio K_{rc}/K_B. In this paper, the rotational stiffness ratio is defined as K_{rP}/K_B including the influence of the axial load P (Figure 14).

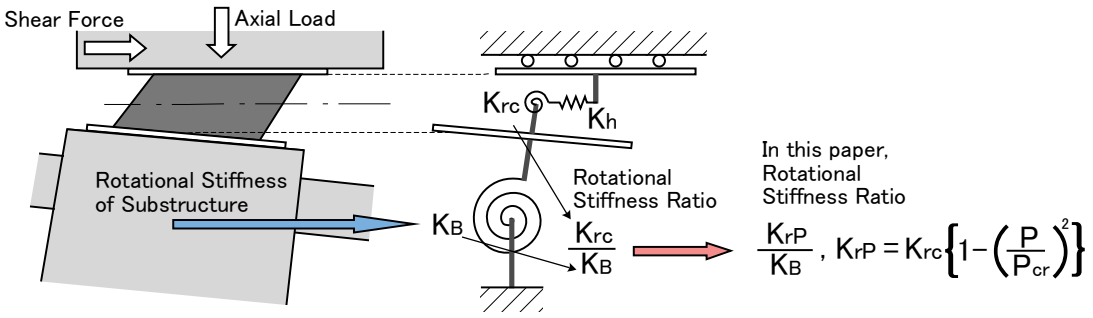

Fig.14 – Outline of rotational stiffness ratio

From the results of all dynamic analyses, the values of θ_B / δ could be derived by the least squares method. Figure 15 shows the relationship of θ_B / δ and K_{rP}/K_B. As shown in Figure 16, the rotational stiffness K_B of the substructure is derived as the equivalent rotational stiffness from $\theta_{\max}$ by dynamic analysis and the $M - \theta$ curve obtained from static analysis using the analytical model of the substructure. As shown in Figure 15,

because the high correlation between the two can be seen, it can be understood that they have a linearly proportional relationship.

Therefore, K_{rP}/K_B can be considered an indicator that correspond to θ_B/δ. By using the results of dynamic analyses, the relationship of K_{rP}/K_B and K_{eq}/K_h (shown in Figure 9) is shown in Figure 17. As shown in this figure, it can be understood that K_{eq}/K_h can be predicted using the rotational stiffness ratio K_{rP}/K_B, because K_{rP}/K_B and K_{eq}/K_h have a linearly proportional relationship. For example, if you want to design the reduction rate of K_{eq}/K_h to be less than 10%, the value of K_{rP}/K_B must be less than ~0.3.

Next, the distribution ratio α_M of the bending moment of the laminated rubber bearing is studied using the rotational stiffness ratio. As seen from Eq.(15), the values of not only θ_B/δ but also ϕ_{rc} and ϕ_σ are unknown. Therefore, for the distribution ratio α_M, Eq.(16) is considered an indicator (because the influence of ϕ_σ is small, only ϕ_{rc} is considered). The horizontal deformation x input to ϕ_{rc} is the maximum horizontal deformation $\delta_{\max}$ of the laminated rubber bearing in the dynamic analysis.

$$\frac{\phi_{rc}(\delta_{\max})\cdot K_{rP}}{K_B} \tag{16}$$

By using the results of dynamic analysis, the relationship of Eq.(16) and α_M (shown in Figure 12) is shown in Figure 18. As shown in this figure, α_M can be predicted using Eq.(16) because they have a linearly proportional relationship.

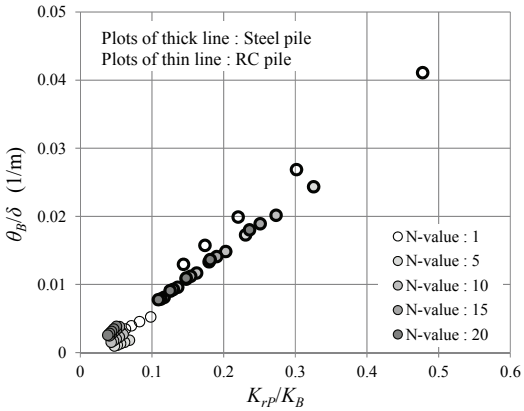

Fig.15 – Relationship of θ_B/δ and K_{rP}/K_B

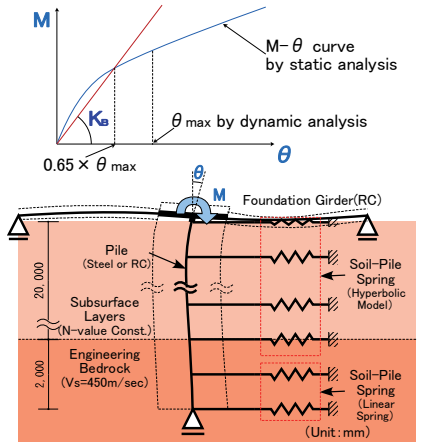

Fig.16 – Rotational stiffness K_B by static analysis

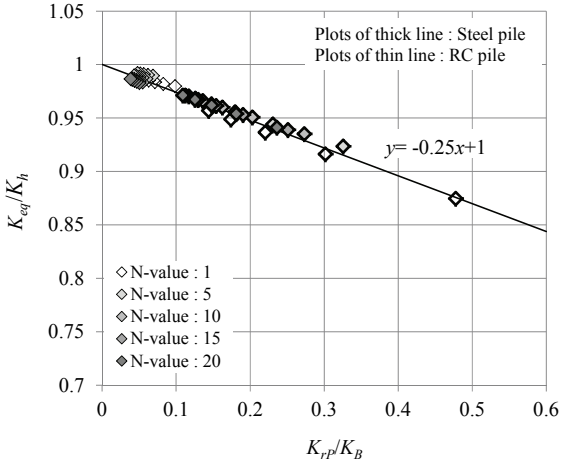

Fig.17 – Relationship of K_{eq}/K_h and K_{rP}/K_B

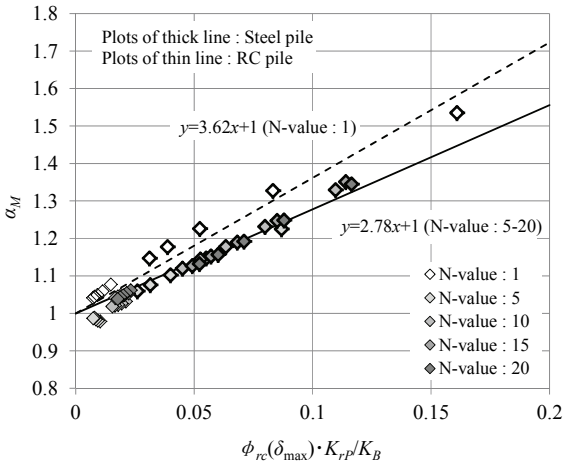

Fig.18 – Relationship of α_M and $\phi_{rc}(\delta_{\max})\cdot K_{rP}/K_B$

4.2 Dependency of Axial Load

Eqs.(12) and (15) both contain the axial load P, and they reveal the dependency of the axial load. Therefore, dynamic analysis is performed using the same conditions as those described previously by setting two different axial loads: 6000 kN (axial stress: 7.6 N/mm^2) and 10000 kN (axial stress: 12.7 N/mm^2).

By using the results of dynamic analysis, the relationship of K_{rP}/K_B and K_{eq}/K_h is shown in Figure 19, and the relationship of Eq.(16) and α_M is shown in Figure 20. As shown in Figure 19, when the axial load P is large, the reduction rate of K_{eq}/K_h is large. This can be understood from Eq.(12). On the other hand, as shown in Figure 20, when the axial load P is large, the value of α_M is small. Considering Eq.(15), this phenomenon is considered to occur because the decrease in α_M occurs with the increase in the axial load P.

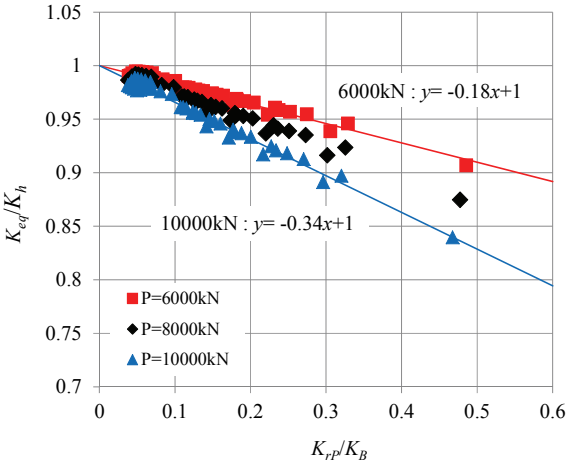

Fig.19 – Relationship of K_{eq}/K_h and K_{rP}/K_B (Dependency of axial load)

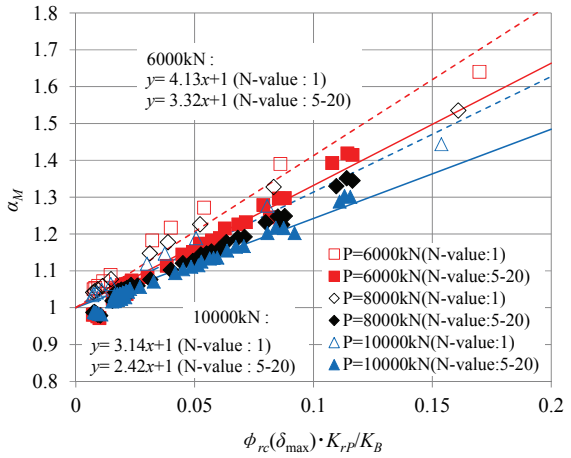

Fig.20 – Relationship of α_M and $\phi_{rc}(\delta_{\max})\cdot K_{rP}/K_B$ (Dependency of axial load)

5. Conclusion

In this paper, the dynamic characteristics of laminated rubber bearings in a pile top seismic isolation building are quantitatively evaluated through earthquake response analysis.

The following conclusions are obtained through numerical experiments using the analytical model considering the nonlinearity of the laminated rubber bearing and the dynamic soil–structure interaction.

1) K_{eq}/K_h and α_M are quantitatively evaluated depending on the characteristics of the substructure. In addition, it is shown that their values are affected by the influence of the correlation between the horizontal deformation and the rotational angle of the laminated rubber bearing.

2) It is clarified that K_{eq}/K_h and α_M can be evaluated using a simple indicator called the rotational stiffness ratio. In addition, their values are evaluated by considering the dependency of the axial load on the laminated rubber bearing.

6. References

[1] M. Kobayashi, S. Shimoda, T. Nishimura (2012): A study on lateral stiffness and design stress of install member on laminated rubber bearings subjected to end rotation. *Journal of Structural and Construction Engineering (Architectural Institute of Japan)*, Vol.77, No.682, 1873-1880, Japan.

[2] T. Miyama (2002): Study on the force-deformation relationships of base-isolation rubber bearing with forced rotation angles at their top and bottom ends. *Journal of Structural and Construction Engineering (Architectural Institute of Japan)*, No.556, 43-50, Japan.

[3] M. Iizuka (1995): Stiffness matrix of laminated rubber bearing (Formulation based on Haringx's theory). *Summaries of Technical Papers of Annual Meeting (Architectural Institute of Japan)*, B-2, 619-620, Japan.

[4] Architectural Institute of Japan (2010): AIJ standard for structural calculation of reinforced concrete structures. Japan.

[5] Architectural Institute of Japan (2005): Design standard for steel structures -Based on allowable stress concept-. Japan.

[6] Japan Road Association (2012): Specifications for highway bridges Part V seismic design. Japan.

[7] Architectural Institute of Japan (2006): Seismic response analysis and design of buildings considering dynamic soil-structure interaction. Japan.

[8] K. Ishihara, N. Yoshida, S. Tsujino (1985): Modelling of stress-strain relations of soils in cyclic loading. *Fifth International Conference on Numerical Methods in Geomechanics Nagoya*, 373-380.

[9] K. Koyamada, Y. Miyamoto, K. Miura (2003): Nonlinear property for surface strata from natural soil samples. *38th Japan National Conference on Geotechnical Engineering (The Japanese Geotechnical Society)*, 2077-2078, Japan.

[10] J. A. Haringx (1948, 1949): On highly compressible helical springs and rubber rods and their application for vibration-free mountings I, II, III. *Philips Research Reports*, Vol.3-4.

[11] T. Nishimura, K. Watanabe (2010): Evaluations of analytical models on rotational characteristics of rubber bearings for 3D dimensional seismic isolation device. *Technical Research Report of Shimizu Corporation*, Vol.87, 19-25, Japan.